Discovery of the elusive radical NCO and confirmation of H₂NCO⁺ in space★

N. Marcelino[1], **M. Agúndez**[1], **J. Cernicharo**[1], **E. Roueff**[2], and **M. Tafalla**[3]

[1]Instituto de Física Fundamental, CSIC, C/ Serrano 123, 28006 Madrid, Spain

[2]Sorbonne Université, Observatoire de Paris, Université PSL, CNRS, LERMA, F-92190, Meudon, France

[3]Observatorio Astronómico Nacional (OAN), C/ Alfonso XII 3, 28014 Madrid, Spain

Abstract

The isocyanate radical (NCO) is the simplest molecule containing the backbone of the peptide bond, C(=O)-N. This bond has a prebiotic interest since is the one linking two amino acids to form large chains of proteins. It is also present in some organic molecules observed in space such as HNCO, NH_2CHO and CH_3NCO. In this letter we report the first detection in space of NCO towards the dense core L483. We also report the identification of the ion H_2NCO^+, definitively confirming its presence in space, and observations of HNCO, HOCN, and HCNO in the same source. For NCO, we derive a column density of 2.2×10^{12} cm^{-2}, which means that it is only ~5 times less abundant than HNCO. We find that H_2NCO^+, HOCN and HCNO have abundances relative to HNCO of 1/400, 1/80, and 1/160, respectively. Both NCO and H_2NCO^+ are involved in the production of HNCO and several of its isomers. We have updated our previous chemical models involving NCO and the production of the CHNO isomers. Taking into account the uncertainties in the model, the observed abundances are reproduced relatively well. Indeed, the detection of NCO and H_2NCO^+ in L483 supports the chemical pathways to the formation of the detected CHNO isomers. Sensitive observations of NCO in sources where other molecules containing the C(=O)-N subunit have been detected could help in elucidating its role in prebiotic chemistry in space.

Keywords

1 Introduction

Most molecules observed in space can be formed with just four atoms, H, C, N, and O. These atoms are the building blocks of organic and prebiotic molecules, and arranged together, constitute the backbone of the peptide bond R–C(=O)–N(–H)–R′, which links two

amino acids and allows to build large proteins. Therefore, the observation of simple molecules with the C(=O)–N group in space can provide important clues on the earliest chemical steps in the synthesis of amino acids. The isocyanate radical (NCO) is the simplest such species and it is predicted to be abundant in dark clouds (Prasad & Huntress 1978; Marcelino et al. 2009). It is also the main precursor of isocyanic acid (HNCO), a species that has been found in a large variety of interstellar environments (see Marcelino et al. 2009, and references within).

HNCO has several metastable isomers: HOCN, HCNO, and HONC, which lie respectively at 24.7, 70.7, and 84.1 kcal mol^{-1} respect to HNCO (see Schuurman et al. 2004). Two of these isomers, HCNO and HOCN, have also been previously detected in molecular clouds (Marcelino et al. 2009, 2010; Brünken et al. 2010). The chemical pathways to the formation of these species are diverse, but the main precursors in gas-phase are the radicals NCO and CNO (Marcelino et al. 2010; Quan et al. 2010). Followed by protonation and hydrogenation, these radicals will lead to the different protonated CHNO ions: H_2NCO^+, $HNCOH^+$, $HCNOH^+$, H_2OCN^+, and H_2CNO^+ (Marcelino et al. 2010; Quan et al. 2010). By dissociative recombination reactions, these ions could produce all the CHNO isomers, including the highest isomer in energy HONC not detected so far in space, and also the NCO radical (Marcelino et al. 2010). The two isomeric forms of the protonated isocyanic acid H_2NCO^+ and $HNCOH^+$, have been studied in the laboratory (Lattanzi et al. 2012; Gupta et al. 2013), and H_2NCO^+ has been tentatively detected in absorption of the low-lying rotational transitions in the centimeter band towards the molecular cloud Sgr B2(N) by Gupta et al. (2013).

In this letter, we report the first detection in space of NCO and we confirm the presence of H_2NCO^+ through millimeter emission transitions. These species were detected towards L483, a dense core located in the Aquila Rift which hosts a protostar, IRAS 18148–0440, in transition from Class 0 to Class I and which shows infall motions and a collimated molecular outflow (Tafalla et al. 2000; Park et al. 2000). Based on the bright emission of carbon chains like C_4H (Agúndez et al. 2008; Sakai et al. 2009), it has been suggested that L483 may host a warm-carbon-chain-chemistry environment. Apart from carbon chains, L483 is also rich in O-bearing organic molecules such as HCO, HCCO, H_2CCO, CH_3CHO, HCCCHO, and c-C_3H_2O (Agúndez et al. 2015a; Loison et al. 2016). Recently, the chemical richness of the source has been evidenced with the discovery of several new molecules: HCCO, $NCCNH^+$, NS^+, HCS, and HSC (Agúndez et al. 2015a,b, 2018; Cernicharo et al. 2018). Recent ALMA observations have shown a chemical differentiation in L483, with carbon chains such as C_2H tracing the envelope and more complex organics like HNCO, NH_2CHO, and $HCOOCH_3$ being distributed around the protostar (Oya et al. 2017). The detection of NCO and H_2NCO^+ around a low-mass protostar such as L483 can thus shed light on the formation of prebiotic molecules containing the C(=O)–N group, like HNCO and its isomers, NH_2CHO, and CH_3NCO (Cernicharo et al. 2016; Quénard et al. 2018).

2 Observations

The data presented here are part of a full 3 mm (80-116 GHz) spectral line survey of L483, using the IRAM 30m radiotelescope in Granada (Spain). The line survey observations were

performed in several sessions, in August and November 2016, and in May and December 2017. We also obtained Director's Discretionary Time to confirm the detection of NCO and H_2NCO^+ in January 2018. The observed position corresponds to that of the infrared source IRAS 18148–0440, $\alpha_{J2000} = 18^h17^m29.8^s$ and $\delta_{J2000} = -04°39'38.0''$ (Fuller & Myers 1993).

We used the EMIR receivers operating at 3 mm, connected to the Fast Fourier Transform Spectrometers (FTS) in high resolution mode, providing a spectral resolution of 50 kHz, which corresponds to velocity resolutions of ~0.13–0.19 km s^{-1} in the 80-116 GHz range. Thanks to the versatility of the EMIR and FTS, we could observe 4 different bands per spectral setup covering 4×1.8 GHz of bandwidth. All the observations were done in Frequency Switching mode, with a frequency throw of 7.2 MHz. Pointing and Focus were checked every 1 and 3 hours, respectively. Pointing errors were always within 3$''$. The 30 m beam sizes at 3 mm are between 30$''$ and 21$''$. Weather conditions were different from one observing period to other, ranging from good winter conditions, with 2-5 mm of precipitable water vapor (pwv), to average summer conditions, with pwv 10 mm. Concerning the data presented here, system temperatures range between 90 and 120 K and the final rms noise is ~1-4 mK, depending on frequency. The spectra were calibrated in antenna temperature corrected for atmospheric attenuation and for antenna ohmic and spillover losses using the ATM package (Cernicharo 1985; Pardo et al. 2001). Data reduction and analysis were done using the CLASS program of the GILDAS software[1].

3 Results

During the analysis of the spectral survey data, we have found a number of unidentified lines. Among them there are several features at 81.4 GHz and 104.6 GHz which are coincident with the strongest components of the $J = 7/2 – 5/2$ and $J = 9/2 – 7/2$ transitions of the NCO radical in the $^2\Pi_{3/2}$ state (see Figure 1). The radical NCO is a linear triatomic molecule with a $^2\Pi_i$ electronic ground state, where the $^2\Pi_{1/2}$ spin-orbit state lies 137 K above the $^2\Pi_{3/2}$ state. The rotational levels are split by Λ doubling, leading to e and f parities, and are further split due to the interaction with the nuclear spin of ^{14}N, leading to a hyperfine structure (Saito & Amano 1970; Kawaguchi et al. 1985; see also CDMS[2]; Müller et al. 2005, and MADEX[3]; Cernicharo 2012). Already in 1978, this radical was predicted to be abundant in dark clouds (Prasad & Huntress 1978), although it has not been yet detected in space probably because of its low dipole moment (0.64 D, Saito & Amano 1970). The complex rotational spectrum of NCO helps in the assignment of the lines. The strongest components of the $J = 7/2 – 5/2$ and $J = 9/2 – 7/2$ are detected in L483, with no missing line, and with center frequencies and relative intensities in very good agreement with the values obtained from laboratory. With the identification of 12 different transitions, the detection of NCO can be considered secure.

We have also detected six lines arising from H_2NCO^+, the lowest energy isomer of protonated isocyanic acid (see Figure 2). This ion has a large dipole moment (4.13 D,

[1]http://www.iram.fr/IRAMFR/GILDAS
[2]http://www.astro.uni-koeln.de/cdms/
[3]https://nanocosmos.iff.csic.es/?page_id=1619

Lattanzi et al. 2012) and has been tentatively detected towards the molecular clouds in the Galactic Center Sgr B2(N) in absorption at 20 and 40 GHz by Gupta et al. (2013). H_2NCO^+ is a planar molecular ion with a C_{2v} symmetry, in which the two H nuclei are equivalent. Thus, the rotational levels are separated into *ortho* (K_a odd) and *para* (K_a even) states, with statistical weights 3:1. Due to the ^{14}N nuclear spin, H_2NCO^+ also presents quadrupole hyperfine structure. However it is unresolved in the L483 spectra (see Fig. 2) and we do not take it into account in the analysis below. Although the lines of H_2NCO^+ in L483 are weak, with T_A^* between 5 and 10 mK, all of them are detected above the 3σ level (rms noise levels are 1.2-2 mK). Furthermore, the fact that all the strongest transitions covered in the 3 mm band are detected, well centered at the systemic velocity of L483 ($V_{LSR} \sim 5.3$ km s^{-1}; Fuller & Myers 1993; Agúndez et al. 2008), supports the identification.

Table A.1 lists all the observed transitions, together with the line parameters derived from gaussian fits. Rest frequencies and spectroscopic data were taken from the MADEX catalogue (Cernicharo 2012). We have computed column densities assuming Local Thermodynamic Equilibrium (LTE) and $T_{rot} = 10$ K, which is consistent with the values obtained for other species in this cloud (Agúndez et al. 2015a,b). For NCO, since the range of upper level energies covered by the observed transitions is narrow (6.6-11.7 K; see Table A.1), the rotational temperature is poorly constrained using rotational diagrams. In the case of H_2NCO^+, we have a relatively low number of transitions available when considering *ortho* and *para* species separately (in particular only two transitions are observed for the *para* state). Derived column densities are $N = (2.2 \pm 0.7) \times 10^{12}$ cm^{-2} for NCO, and 3.0×10^{10} cm^{-2} for H_2NCO^+ (values for the *ortho* and *para* species are $(2.1 \pm 0.5) \times 10^{10}$ cm^{-2} and $(8.6 \pm 3.9) \times 10^9$ cm^{-2}, respectively). In the line survey we have also covered two transitions of HNCO, HOCN and HCNO. We have computed column densities for all these species assuming $T_{rot} = 10$ K. The fourth isomer, HONC, and the ion $HNCOH^+$ are not detected, and hence only upper limits are provided. The column densities and fractional abundances derived are listed for all species in Table 1. We used $N(H_2) = 3 \times 10^{22}$ cm^{-2}, which was derived by Tafalla et al. (2000) from observations of $C^{17}O$.

4   Discussion

The chemical processes linking H, C, O and N atoms take place in combustion processes but the kinetics at the low temperatures of interstellar clouds is subject to many uncertainties. To investigate the formation of NCO and H_2NCO^+ in L483, we have updated the chemical schema used in Marcelino et al. (2009, 2010) by considering the UMIST (McElroy et al. 2013) and KIDA (Wakelam et al. 2015) databases. In the absence of experimental or theoretical information on the kinetics, we have verified the energy balance of various reactions. Table A.2 reports our estimate of the formation enthalpies of different isomers of the $CHNO^+$ and CH_2NO^+ ions, which are not all reported in thermodynamic tables nor in the KIDA database. We find that some reactions suggested in KIDA are in fact endothermic, e.g.,

$$HOCN^+ + H_2 \rightarrow H_2OCN^+ + H, \quad (1)$$

$$HCNO^+ + H_2 \rightarrow H_2CNO^+ + H. \quad (2)$$
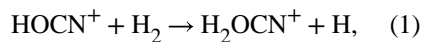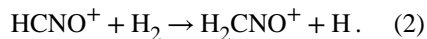
It is obvious that our tentative chemical network is subject to many uncertainties. Amongst these, the dissociative recombination (DR) rate coefficients of the CH_2NO^+ ions and the branching ratios are quite critical. The present model results are obtained when ejection of H and H_2 are favoured compared to other neutral channel products. In the cases where two CHNO isomers are produced in the DR, we have also assumed that the most stable is produced preferentially. The corresponding reaction rate coefficients are displayed in Table A.3. Another uncertainty in our chemical network is the formation route of H_2NCO^+ through the $NH_3 + HCO^+$ reaction, which is exothermic. For this channel we assume a rate coefficient of $2.5 \times 10^{-10}(T/300)^{-0.5}$ cm^3 s^{-1}, while for the rapid proton transfer channel leading to $NH_4^+ + CO$ we consider a higher rate coefficient of $2.2 \times 10^{-9}(T/300)^{-0.5}$ cm^3 s^{-1}.

In Fig. 3 we show the time evolution of the abundances of various species of interest, as given by our gas-phase chemical model. We have adopted a H_2 volume density of 3.4×10^4 cm^{-3} and a gas kinetic temperature of 10 K, which are adequate for the L483 cloud (Fuller & Myers 1993; Anglada et al. 1997; Jørgensen et al. 2002). The cosmic ionization rate is fixed to 1.3×10^{-17} s^{-1} and the elemental abundances of C, N, O, S relative to hydrogen are set to 9×10^{-6}, 1×10^{-5}, 1.5×10^{-5} and 2×10^{-8}, respectively. The relative abundances for the detected species are rather well reproduced by our model, while those of HONC and $HNCOH^+$ are below the observed upper limits. Given the uncertainties of the chemical network, the agreement between the model and the observations is quite satisfactory.

The different species treated in this paper appear to follow different reaction routes, both through neutral-neutral reactions and ion-molecule schema. NCO is formed straightforwardly through the $CN + O_2$ reaction at a reaction rate of 2.4×10^{-11} cm^3 s^{-1} (Glarborg et al. 1998). Fulminic acid (HCNO), despite at an energy of about 68 kcal mol^{-1} above the most stable isomer HNCO, is one of the main products, together with HCN, of the reaction between CH_2 and NO, as found in the laboratory (Grussdorf et al. 1994) and explained theoretically (Roggenbuck & Temps 1998). HNCO and HOCN, on the other hand, are rather formed through ion molecule schema as products in the dissociative recombination of H_2NCO^+ and $HNCOH^+$, although the reaction for the latter has not yet been studied in the laboratory. The detection of H_2NCO^+ validates the occurrence of the ion-molecule formation schema.

5   Conclusions

In this letter we report the first detection in space of the NCO radical with a significant abundance, only ~5 times lower than HNCO, towards the low-mass protostar L483. Together with H_2NCO^+, detected as well in this dense core, they are involved in the production of HNCO and some of its isomers. In L483 we obtain similar abundances of HOCN and HCNO, which is consistent with what was found by Marcelino et al. (2010) in dense cores. It is possible that NCO and H_2NCO^+ could be present in these sources as well.

Unfortunately the corresponding frequencies were either not covered or the available data were not sensitive enough. Observations of NCO in sources at different stages across the star formation process could help to dilucidate its role in the synthesis of CHNO isomers and prebiotic molecules containing the C(=O)–N group.

Supplementary Material

Refer to Web version on PubMed Central for supplementary material.

Acknowledgements

References

Agúndez M, Cernicharo J, Guélin M, et al. A&A. 2008; 478:L19.

Agúndez M, Cernicharo J, Guélin M. A&A. 2015a; 577:L5.

Agúndez M, Cernicharo J, de Vicente P, et al. A&A. 2015b; 579:L10.

Agúndez M, Marcelino N, Cernicharo J, Tafalla M. A&A. 2018; 611:L1.

Anglada G, Sepúlveda I, Gómez JF. A&AS. 1997; 121:255.

Brünken S, Belloche A, Martín S, Verheyen L, Menten KM. A&A. 2010; 516:A109.

Cernicharo, J. Internal IRAM report. Granada: IRAM; 1985.

Cernicharo, J. In: Stehlé, C.Joblin, C., d'Hendecourt, L., editors. ECLA-2011: Proc. of the European Conference on Laboratory Astrophysics, EAS Publications Series; Cambridge: Cambridge Univ. Press; 2012.

Cernicharo J, Kisiel Z, Tercero B, et al. A&A. 2016; 587:L4.

Cernicharo J, Lefloch B, Agúndez M, et al. A&A. 2018; 853:L22.

Fuller GA, Myers PC. ApJ. 1993; 418:273.

Glarborg P, Alzueta MU, Dam-Johansen K, Miller JA. Combustion and Flame. 1998; 115:1.

Grussdorf J, Nolte J, Temps F, Wagner HG. Ber Bunsenges Phys Chem. 1994; 98:546.

Gupta H, Gottlieb CA, Lattanzi V, Pearson JC, McCarthy MC. ApJ. 2013; 778:L1.

Ijjaali F, Alcami M, Mó O, Yáñez M. Mol Phys. 2001; 99:1129.

Jørgensen JK, Schöier FL, van Dishoeck EF. A&AS. 2002; 389:908.

Kawaguchi K, Saito S, Hirota E. Mol Phys. 1985; 55:341.

Lattanzi V, Thorwirth S, Gottlieb CA, McCarthy MC. J Phys Chem Lett. 2012; 3:3420. [PubMed: 26290966]

Lias SG, Liebman JF, Levin RD. J Phys Chem Ref Data. 1984; 13:695.

Loison J-C, Agúndez M, Marcelino N, et al. MNRAS. 2016; 456:4101.

Luna A, Mebel AM, Morokuma K. J Chem Phys. 1996; 105:3187.

Marcelino N, Cernicharo J, Tercero B, Roueff E. ApJ. 2009; 690:L27.

Marcelino N, Brünken S, Cernicharo J, et al. A&A. 2010; 516:A105.

McElroy D, Walsh C, Markwick AJ, et al. A&A. 2013; 550:A36.

Müller HSP, Schlöder F, Stutzki J, Winnewisser G. J Mol Struct. 2005; 742:215.

Oya Y, Sakai N, Watanabe Y, et al. ApJ. 2017; 837:174.

Pardo JR, Cernicharo J, Serabyn E. IEEE Trans Antennas Propag. 2001; 49:12.

Park Y-S, Panis J-F, Ohashi N, et al. ApJ. 2000; 542:344.

Prasad SS, Huntress WT Jr. MNRAS. 1978; 185:741.

Quan D, Herbst E, Osamura Y, Roueff E. ApJ. 2010; 725:2101.

Quénard D, Jiménez-Serra I, Viti S, Holdship J, Coutens A. MNRAS. 2018; 474:2796.

Roggenbuck J, Temps F. Chemical Physics Letters. 1998; 285:422.

Saito S, Amano T. J Mol Spectrosc. 1970; 34:383.

Sakai N, Sakai T, Hirota T, et al. ApJ. 2009; 697:769.

Schuurman MS, Muir SR, Allen WD, Shaefer HF III. 2004; 120:11586.

Tafalla M, Myers PC, Mardones D, Bachiller R. A&A. 2000; 359:967.

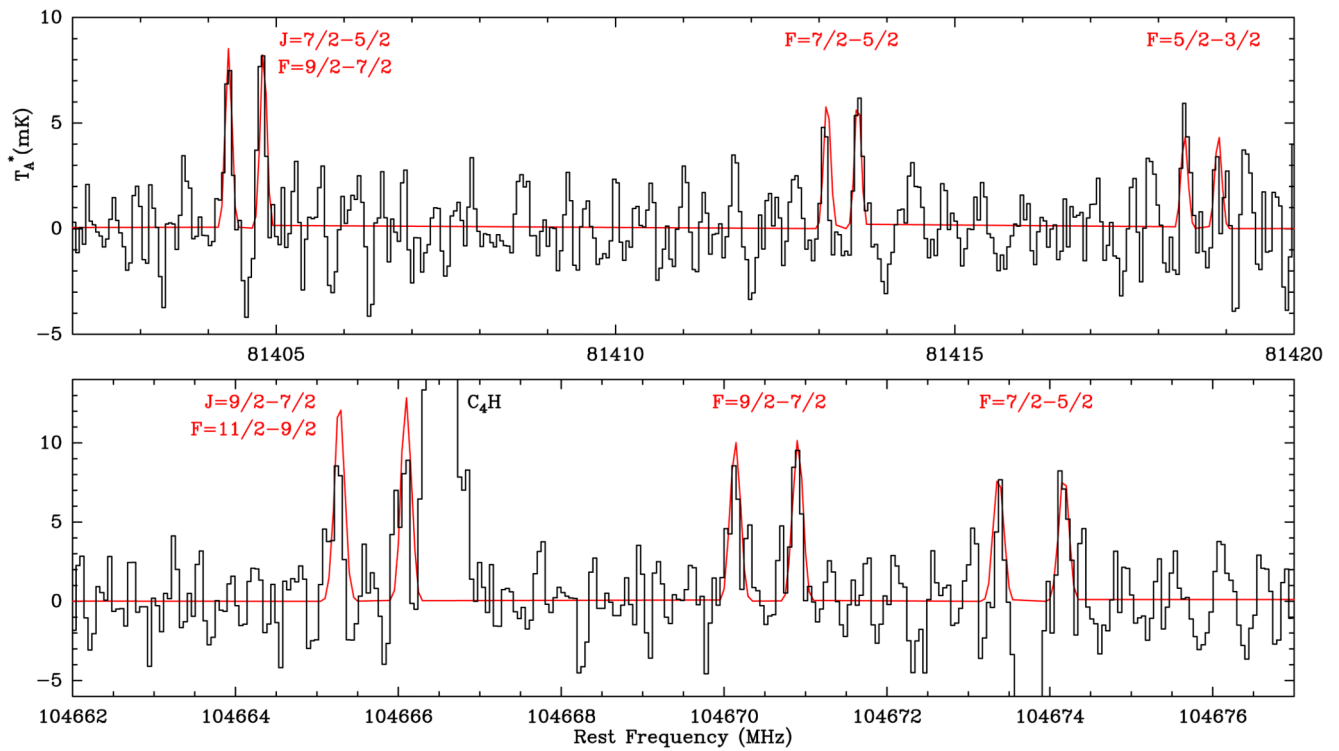Wakelam V, Loison J-C, Herbst E, et al. ApJS. 2015; 217:20.

Fig. 1.

Observed transitions of NCO in the $^2\Pi_{3/2}$ state towards L483. The strongest components of the $J = 7/2 - 5/2$ and $J = 9/2 - 7/2$ transitions are shown in the upper and lower panels, respectively. LTE results are overplotted in red. Note that the absorption feature in the lower panel between the doublet $F = 7/2 - 5/2$ is not real, it is the corresponding negative of the C_4H line due to the Frequency Switching observing mode (located 7.2 MHz away).
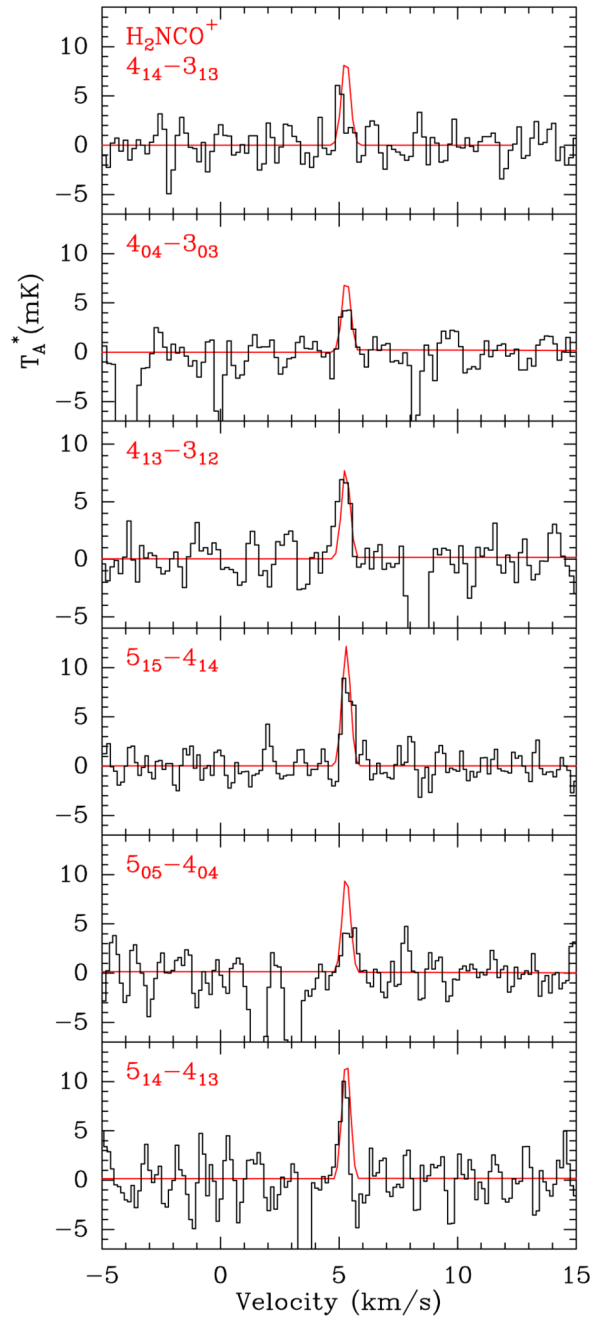
Fig. 2.
Observed transitions of H_2NCO^+ towards L483. LTE results are overplotted in red.
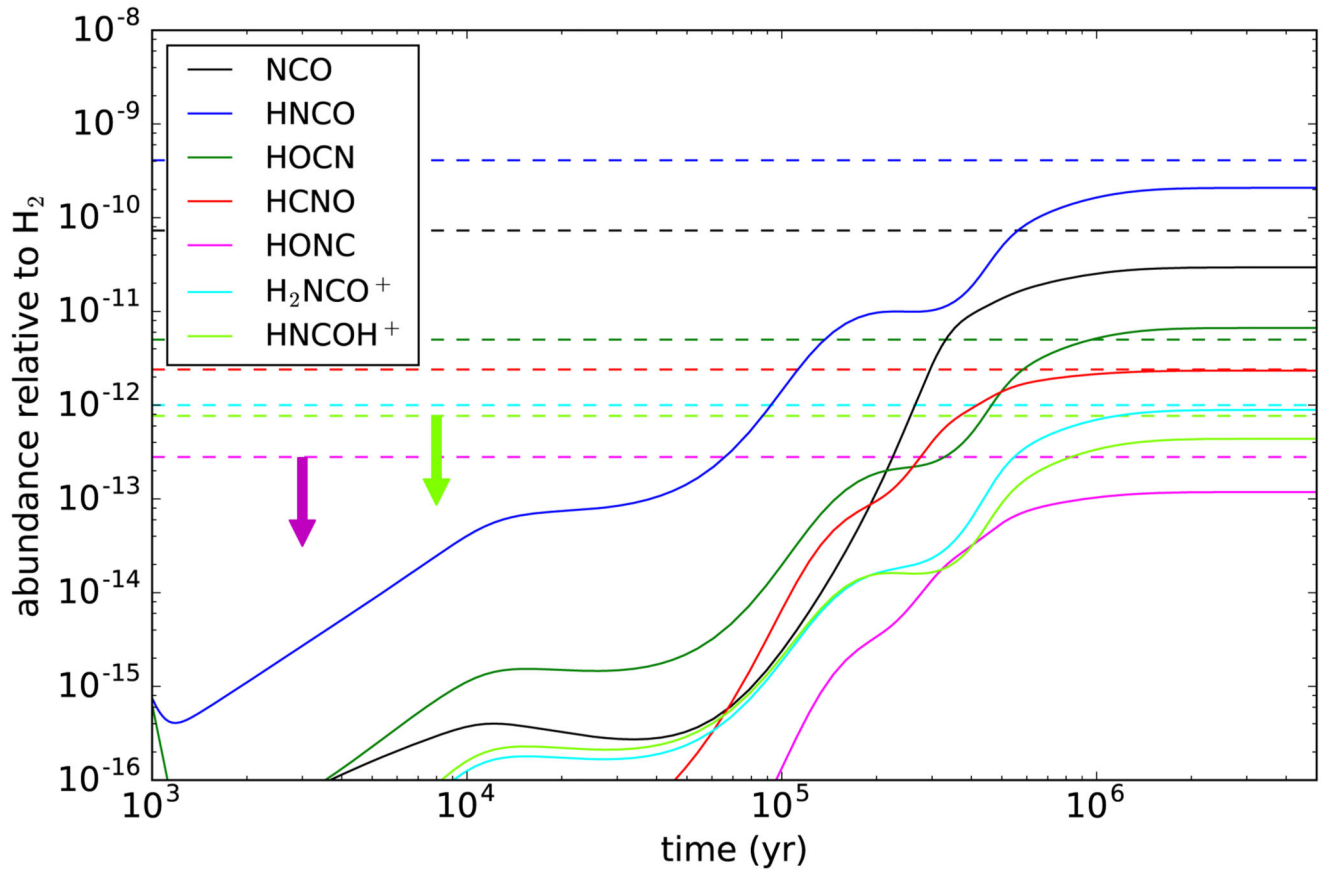
Fig. 3.
Fractional abundances calculated as a function of time with our chemical model (see text).
Horizontal dashed lines indicate the abundances derived from observations.

Table 1

Column densities and fractional abundances derived.

Species	N (cm^{-2})	X/H$_2$	HNCO/X
NCO	2.2×10^{12}	7.3×10^{-11}	5.5
H$_2$NCO$^+$	3.0×10^{10}	1.0×10^{-12}	400
HNCOH$^+$	$<2.3 \times 10^{10}$	$<7.7 \times 10^{-13}$	>520
HNCO	1.2×10^{13}	4.1×10^{-10}	–
HOCN	1.5×10^{11}	5.0×10^{-12}	80
HCNO	7.3×10^{10}	2.4×10^{-12}	160
HONC	$<8.3 \times 10^{9}$	$<2.8 \times 10^{-13}$	>1450